THE JOURNAL OF BIOLOGICAL CHEMISTRY VOL. 287, NO. 31, pp. 25727–25740, July 27, 2012

Involvement of the Up-regulated FoxO1 Expression in Follicular Granulosa Cell Apoptosis Induced by Oxidative Stress*[S]

Received for publication, February 6, 2012, and in revised form, May 24, 2012 Published, JBC Papers in Press, June 4, 2012, DOI 10.1074/jbc.M112.349902

Ming Shen[‡], Fei Lin[‡], Jiaqing Zhang[‡], Yiting Tang[‡], Wei-Kang Chen[§1], and Honglin Liu[‡2]

From the [‡]College of Animal Science and Technology, Nanjing Agricultural University, Nanjing 210095, China and [§]K & R BioPharmaceuticals, 60 Jiangsu Road, Building C Suite 2203, Nanjing 210009, China

Background: Granulosa cell (GC) apoptosis is the main cause of follicular atresia, and oxidative stress is involved in this process.
Results: GC apoptosis is caused by FoxO1 activity in oxidative stress.
Conclusion: FoxO1 is critical in oxidative stress-induced GC apoptosis.
Significance: Our results detail the mechanism of follicular atresia and indicate that FoxO1 is a potential target in preventing follicular atresia from oxidative stress.

Follicular atresia is common in female mammalian ovaries, where most follicles undergo degeneration at any stage of growth and development. Oxidative stress gives rise to triggering granulosa cell apoptosis, which has been suggested as a major cause of follicular atresia. However, the underlying mechanism by which the oxidative stress induces follicular atresia remains unclear. FoxO transcription factors are known as critical mediators in the regulation of oxidative stress and apoptosis. In this study, the involvement of FoxO1 in oxidative stress-induced apoptosis of mouse follicular granulosa cells (MGCs) was investigated *in vivo* and *in vitro*. It was observed that increased apoptotic signals correlated with elevated expression of FoxO1 in MGCs when mice were treated with the oxidant. Correspondingly, the expressions of FoxO1 target genes, such as proapoptotic genes and antioxidative genes, were also up-regulated. In primary cultured MGCs, treatment with H_2O_2 led to FoxO1 nuclear translocation. Further studies with overexpression and knockdown of FoxO1 demonstrated the critical role of FoxO1 in the induction of MGC apoptosis by oxidative stress. Finally, inactivation of FoxO1 by insulin treatment confirmed that FoxO1 induced by oxidative stress played a pivotal role in up-regulating the expression of downstream apoptosis-related genes in MGCs. Our results suggest that up-regulation of FoxO1 by oxidative stress leads to apoptosis of granulosa cells, which eventually results in follicular atresia in mice.

Although there are numerous follicles in the ovaries of mammalians, most of them undergo degeneration during growth and development. This process is known as follicular atresia. Follicles consist of granulosa cells, theca internal cells and oocytes. Recent studies suggest that granulosa cell apoptosis is the main cause of follicular atresia, which displays DNA regular degradation, activation of caspases, and enhanced expression of Fas and IGFBP-5 (1–4). Reactive oxygen species (ROS)[3] are highly reactive oxygen groups, which damage cellular components, including DNA, protein, and lipid (5). Generally, ROS are classified into three categories: nonradical ROS hydrogen peroxide (H_2O_2), free oxygen radicals ($O_2^{\cdot-}$) and hydroxyl radicals ($^{\cdot}OH$) (6). These radicals are generated by intracellular sources, such as normal aerobic metabolism, nutrient deprivation, and ischemia, in addition to environmental stress like ionizing radiation or UV (6–7). In fact, ROS are necessary for fundamental cellular processes, such as cell proliferation, survival, and migration (8). However, when ROS are excessively generated, exceeding the eliminative rate, an unbalance between oxidant and antioxidant systems occurs, leading to adverse effects to tissues, a condition known as oxidative stress (9).

Oxidative stress can trigger apoptosis through several pathways. For example, ROS generated by external stimuli, such as H_2O_2, is implicated in most of the growth factor-inducing signaling cascades, including PI3K/Akt, JNK, MAPK, and NF-κB. ROS can activate JNK, NF-κB, and MAPK signaling pathways to trigger apoptosis and/or activate the PI3K/Akt pathway to induce cell survival (5, 10). In mitochondria, H_2O_2, ionizing radiation, or UV elevates the ratio of *Bax*/*Bcl-2* expression, leading to reduced mitochondrial membrane potential, cytochrome *c* release, and caspase-induced apoptosis (11). In endoplasmic reticulum, the oxidative stress-induced endoplasmic reticulum stress activates JNK, CHOP, Bim, Bax, and Bak, impairs Bcl-2, and triggers apoptosis through a mitochondrion-dependent pathway (12).

Oxidative stress-induced apoptosis is believed a major cause of follicular atresia (13). It has been reported that ROS accumulation resulting from mutations in different complexes of the electron transport chain leads to premature ovarian insuffi-

* This work was supported by a grant from a key project of the Chinese National Programs for Fundamental Research and Development (973 Program 2007CB947403).
[S] This article contains supplemental Table S1 and Figs. S1–S6.
[1] To whom correspondence may be addressed. Tel.: 15380895866; E-mail: chen.50@osu.edu.
[2] To whom correspondence may be addressed. Tel.: 86-25-84395106; E-mail: liuhonglin@njau.edu.cn.

[3] The abbreviations used are: ROS, reactive oxygen species; MGC, mouse follicular granulosa cell; 3-NP, 3-nitropropionic acid; qRT-PCR, quantitative RT-PCR; ANOVA, analysis of variance; SOD, superoxide dismutase.

ciency and follicular atresia in human ovary (14). In addition, during follicular atresia, apoptosis and protein oxidation were increased, and GSH glutathione levels were decreased in ewe follicles (15). In contrast, inhibitors of oxidative stress suppress granulosa apoptosis during follicular atresia in rat ovaries (16).

To elucidate the mechanism of oxidative stress and develop corresponding therapeutic tools, various oxidative stress models have been established, including *in vitro* cultured cell models and *in vivo* animal models (17, 18). Several oxidants, such as H_2O_2, D-galactose, nicotine, methoxychlor, and 3-nitropropionic acid (3-NP), have been utilized in rodent models. For example, injection with D-galactose causes a global oxidative injury in rodents (19). Long-term nicotine administration generates serious oxidative damage in rat kidneys (20). Although the methoxychlor agent has been applied to the ovary oxidative stress model in rodents, it is also toxic and causes damage in many tissues (21).

3-NP, a natural organic toxin from some plants and fungus, selectively inhibits succinic dehydrogenase complex (Complex II) in the mitochondrial electron transport chain. Because Complex II is an important linker between the tricarboxylic acid cycle and respiratory chain in the inner mitochondrial membrane, 3-NP structurally resembles succinate and irreversibly binds to Complex II, therefore resulting in a constant inactivation of Complex II (22). Inhibition of Complex II interferes with the electron cascade and interrupts oxidative phosphorylation. Thus, 3-NP may induce a reduction in ATP production and oxidative stress (23–25).

3-NP is also applied as a neurotoxin to simulate neurodegenerative diseases in the rodent model (26), and it has been found that free radicals play a fundamental role in 3-NP-induced neuronal damage (27). High ROS levels were previously detected when rats were intraperitoneally injected with 3-NP (28–30). However, there are few successful reports on the oxidative model specified in mouse ovary studies.

H_2O_2 is widely used as a classical reagent to trigger oxidative stress in cultured cells, which may serve as a useful *in vitro* oxidative stress model (31). H_2O_2 is an important form of active oxygen and is easily accessible across the cell membrane (32). The H_2O_2 treatment generates highly reactive free radicals, which oxidize lipids, proteins, and nucleic acids in cultured cells (33). Due to its reliable effects and relative economy in price, H_2O_2 has become a very popular reagent in studying oxidative stress in different cell types (34).

FoxO (Forkhead O), a subfamily of transcription factors, including FoxO1, FoxO3, FoxO4, and FoxO6, are able to regulate diverse cellular processes that include cell cycle arrest, DNA damage repair, apoptosis, proliferation, differentiation, stress response, senescence, longevity, metabolism, etc. (35–39). As a member of this family, FoxO1 activity is regulated by several exogenous stimuli like growth factors and oxidative stress (40). These stimuli will activate or inactivate FoxO1 by posttranslational modifications and subcellular localization (39). For example, in response to the insulin/IGF-1 signaling activation, the phosphorylated FoxO1 by Akt is able to bind to 14-3-3 protein and to be retrotranslocated from the nucleus to the cytoplasm, where it becomes inactive (41). Conversely, inhibition of the PI3K/Akt pathway results in dephosphorylation and nuclear translocation of FoxO1, which induces cell cycle arrest and apoptosis by up-regulating the expression of the genes, such as cyclin-dependent kinase inhibitor $p27^{KIP1}$, *Bim*, *FasL* (Fas ligand gene), and *TRAIL* (tumor necrosis factor-related apoptosis-inducing ligand gene) (42–46). Also, FoxO1 activity is controlled by acetylation and monoubiquitination (47).

FoxO transcriptional factors are critical regulators in response to oxidative stress. Oxidative states generated by treating cells with H_2O_2 induce nuclear localization of FoxO members (5, 48–49). Much evidence indicates that several kinases are involved in the regulation of the FoxO activity in an oxidative stress condition. For example, JNK phosphorylates FoxO4 at threonines 447 and 451 after H_2O_2 treatment through a small GTPase/Ral-dependent pathway in human colon cancer cells (5, 50). Moreover, the JNK pathway activated by oxidative stress reduces PKB/Akt activity in pancreatic β-cell line HIT cells, resulting in decreased phosphorylation of FoxO1 at threonine 24 and serines 256 and 319 and increasing FoxO1 nuclear localization (50). However, in certain cells, oxidative stress up-regulates the activity of PKB/Akt and SGK, which leads to a negative regulation of FoxO by the nuclear export (41, 51). Therefore, the FoxO activity regulated by different kinases in response to oxidative stress depends on cell types.

FoxO transcriptional factors activated by oxidative stress induce the expression of a series of genes involved in cell cycle arrest, apoptosis, or oxidative stress resistance (39). For example, FoxO1 triggers the expression of apoptosis-related genes, including *Bim*, *FasL*, *Puma*, and *TRAIL*, in response to oxidative stress and induces neuronal death in neurodegenerative diseases (52). In contrast, the activation of FoxO3 protects cells from oxidative stress by up-regulating antioxidant enzymes superoxide dismutase 2 (SOD2) and catalase (53–55). There are additional reports indicating that FoxO factors induce the expression of GADD45α, p130, cyclin D2, p21, and $p27^{Kip1}$, which are involved in cell cycle arrest and DNA repair under oxidative conditions (6, 56–60).

Many studies show the importance of oxidative stress in inducing granulosa cell apoptosis (16). However, it remains to be determined whether FoxO1 is involved in this apoptotic process. In this study, we employed oxidative models to show that oxidant-induced FoxO1 plays a primary role in regulating mouse follicular granulosa cell (MGC) apoptosis. Our results suggest that the oxidative stress in MGCs initiates cell apoptosis by up-regulating the FoxO1 expression and increasing FoxO1 nuclear localization, promoting apoptosis-related gene expression. Such a mechanism of MGC apoptosis eventually may lead to follicular atresia in mice.

EXPERIMENTAL PROCEDURES

Induction of ROS in Vivo—To simulate oxidative stress, female ICR mice (Nanjing Qinglongshan Experimental Animal Center) were injected intraperitoneally with PBS or 3-NP (Sigma). 3-NP was dissolved in PBS to a concentration of 10 mg/ml (pH 7.4) and administered by intraperitoneal injection twice daily for 5 days at a dose of 50 mg/kg (61). All animal experiments were performed according to the guidelines of the regional animal ethics committee.

Measurement of Intracellular ROS—Levels of ROS in cells were measured using the GENMED intracellular ROS red fluorescence determination kit (GENMED, Shanghai, China) and the GENMED cellular superoxide anion colorimetric quantitative determination kit. ROS levels in the brain, liver, kidney, and spleen were detected by the GENMED tissue superoxide anion colorimetric quantitative determination kit. These procedures were performed according to the manufacturer's instructions.

Primary MGC Culture—Mice were injected intraperitoneally with 10 units of PMSG (62) and sacrificed 48 h later. Ovaries were obtained from superovulated mice and transferred into Petri dishes (35 × 15 mm) filled with PBS and then pricked with a syringe under a surgical dissecting microscope to release MGCs. The cell suspensions were put into T75 flasks containing DMEM/F-12 (1:1) with 10% (v/v) fetal bovine serum and incubated at 37 °C with 5% CO_2 for 7 days.

Cell Transfection and Treatments—Plasmids encoding FoxO1 shRNA or scrambled oligonucleotides were ordered from GenePharma (Shanghai, China) (for details, see supplemental Fig. S6). Expression vectors pcDNA3-FLAG-FKHR-(WT) and pcDNA4-FLAG-FKHR(AAA) (see supplemental Fig. S3) were kindly provided by Dr. Haojie Huang (University of Minnesota). For the RNA interference experiment, primary cultured MGCs were transfected with FoxO1 shRNA or corresponding scrambled oligonucleotide control RNA (4 μg/ml) for 6 h using Lipofectamine 2000 (Invitrogen). 24 h later, the cells were treated with H_2O_2 (100 μM) or insulin (100 ng/ml; Sigma) for another 24 h. For an overexpression experiment, MGCs were transfected with pcDNA3-FLAG-FKHR(WT) or pcDNA4-FLAG-FKHR(AAA) (4 μg/ml) using Lipofectamine 2000, and the cells were cultured for 36 h before they were used for the next assay. For an insulin inhibition experiment, MGCs were treated with insulin (100 ng/ml; Sigma) for 24 h, and then the cells were exposed to H_2O_2 (100 μM) for another 24 h. All experiments were repeated in triplicate.

TUNEL Assay—The apoptosis rates were determined by the terminal deoxyribonucleotidyltransferase-mediated dUTP nick end labeling method (63). The detailed procedure was performed according to the protocol of the *In Situ* Cell Death Detection Kit (Roche Applied Science). Images were obtained using a laser-scanning confocal microscope (Zeiss).

Annexin V/Propidium Iodide Assay—For a gain of function test, the cell apoptosis was also identified by an Annexin V/propidium iodide apoptosis kit (KeyGEN, Nanjing, China) according to the manufacturer's instructions. Briefly, the cells grown on coverslips were rinsed with PBS before the phosphatidylserine-exposed cell membrane was visualized by Annexin V-FITC staining at 4 °C for 20 min in a dark place. Then cells were counterstained with propidium iodide at 4 °C for another 5 min. After rinse, the coverslips were mounted on glass slides. Images were taken using a fluorescence microscope (Nikon).

Western Blot Analysis—Total proteins were prepared using radioimmune precipitation assay lysis buffer and quantified by the BCA method (Pierce). 15 μg of total protein/sample was loaded onto a 7.5% SDS-polyacrylamide gel. After electrophoresis, the protein was transferred onto a PVDF membrane (Millipore, Billerica, MA) by electroelution. The membrane was incubated with anti-FoxO1 (catalog no. 1874-1, Epitomics), or anti-FoxO1–256s (catalog no. 9461, Cell Signal Technology) overnight at 4 °C and with HRP-conjugated goat anti-rabbit secondary antibody (catalog no. sc-2030, Santa Cruz Biotechnology, Inc. (Santa Cruz, CA)) for 2 h at 25 °C. After washing, the membrane was processed using SuperSignal West Pico chemiluminescent substrate (Pierce). α-Tubulin, as an internal control, was detected with anti-tubulin antibody (1:1000) (catalog no. T5168, Sigma).

Quantitative RT-PCR (qRT-PCR)—Total RNA was isolated using TRIzol (Invitrogen), and the reactions were performed with Moloney murine leukemia virus RT according to the manufacturer's protocol (Promega). qRT-PCR was performed with SYBR Premix Ex Taq (Takara) in a reaction volume of 20 μl. Primer sequences are listed in supplemental Table S1.

Immunofluorescence Staining—MGCs were grown on coverslips and processed following a standard protocol. Briefly, the cells on coverslips were fixed with 3.7% paraformaldehyde, permeabilized with 0.5% Triton X-100 in PBS, and incubated with anti-FoxO1 antibody (catalog. no. 1874-1) (Genomics), anti-FoxO1-256 (catalog no. 9461, Cell Signal Technology), or anti-FoxO1-319 (catalog no. 2486, Cell Signal Technology) for 1 h at 25 °C. Then the coverslips were incubated with goat anti-rabbit IgG conjugated with Alexa Fluor 488 (green) for another 1 h in a dark place. After the cell nuclei were stained with DAPI for 20 min, the coverslips were finally mounted on glass slides. Fluorescent images were taken using a laser-scanning confocal microscope (Zeiss).

Immunohistology—Mice ovaries were fixed with 4% paraformaldehyde and embedded in paraffin. Sections of ovaries were incubated with anti-FoxO1 (1:100) (catalog no. 1874-1, Genomics) and corresponding secondary antibodies with biotin labeling and then visualized by diaminobenzidie (Sigma). The cell nuclei were counterstained with hematoxylin (Nanjing Jianchen Institute of Biological Engineering, Nanjing, China). In the negative control group, primary antibody was replaced with 1% BSA, and false positive reactivity was not observed in this group.

Statistics—All values are presented as means ± S.E. The statistical significance between groups was analyzed by one-way ANOVA, and values of $p < 0.05$ were considered significant. All experiments were repeated at least three times.

RESULTS

Administration of Oxidant 3-NP Induced Apoptosis in MGCs—FoxO transcription factors are critical regulators in oxidative stress-induced apoptosis. However, the relationship among oxidative stress, FoxO, and apoptosis in follicular MGCs is still unknown. To address this issue, our study began with the measurement of effects of oxidative stress on ROS levels and apoptosis in the MGCs from the oxidative stress-simulated mice.

3-NP is a mitochondrial toxin, which inhibits succinate dehydrogenase and the tricarboxylic acid cycle, resulting in ATP reduction and oxidative stress. High ROS levels were detected previously when rats were intraperitoneally injected with 3-NP (28). Thus, we applied 3-NP as an oxidant to establish an oxidative stress mouse model in our mammal ovary study. With this simulative model, we observed that ROS levels

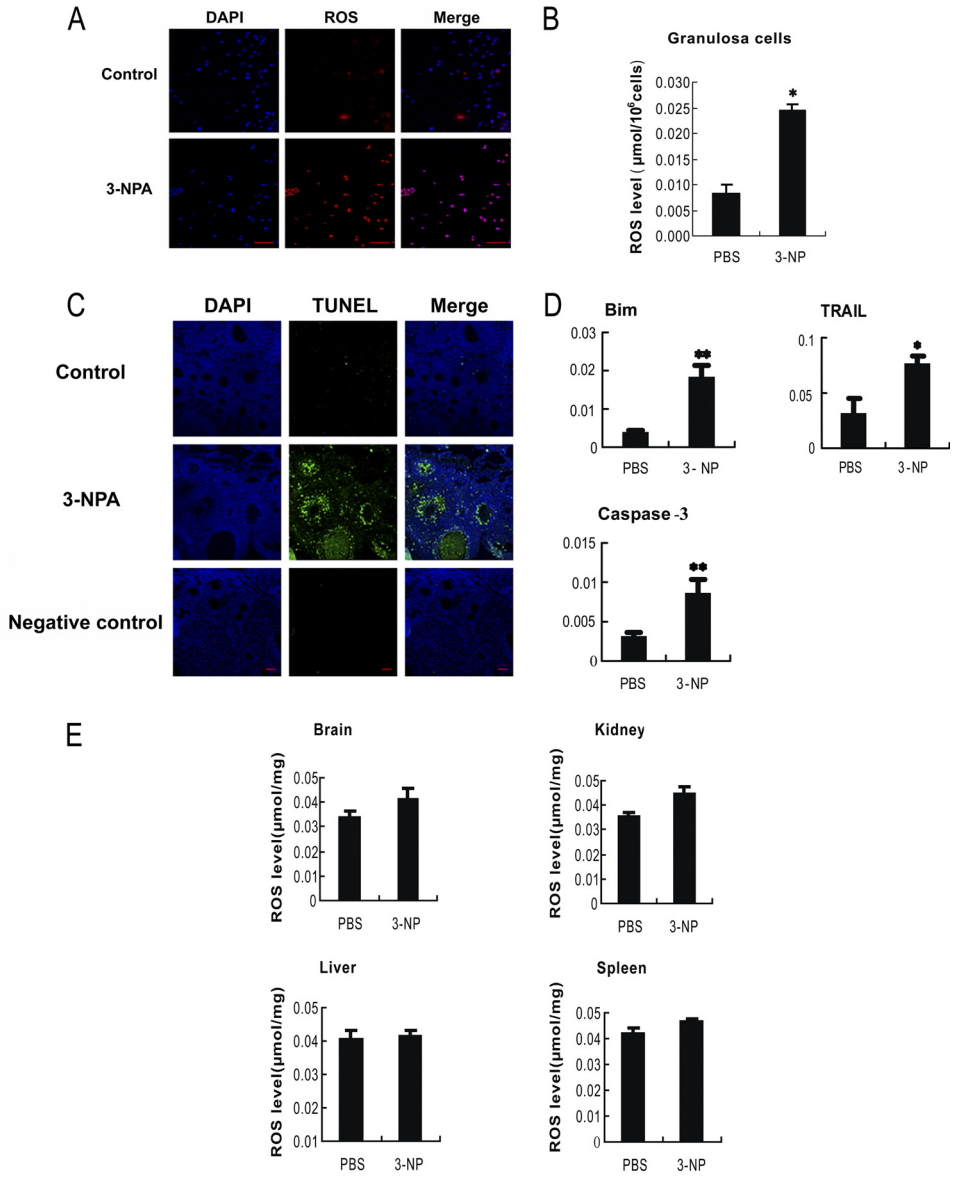

FIGURE 1. **Oxidative stress-induced apoptosis in MGCs.** Mice were intraperitoneally injected with PBS or oxidant 3-NP, respectively. The intracellular ROS in the harvested follicular MGCs (*A*) and from the TUNEL assay of follicular MGCs in the ovary sections (*C*) from intraperitoneally injected mice were measured with a microscope. *Bar*, 50 μm. *B* and *E*, ROS levels in follicular MGCs and several tissues were also quantified by nitro blue tetrazolium (*NBT*) staining. *D*, qRT-PCR showed the induction of apoptosis-related genes in response to oxidant treatments; the relative expression data were normalized to the amount of cellular β-actin. The corresponding data above represent mean ± S.E. (*error bars*) ($n = 3$). The statistical significance between groups was analyzed by one-way ANOVA. *, $p < 0.05$; **, $p < 0.01$.

(Fig. 1, *A* and *B*) and DNA breaks (indicating apoptotic effect) (Fig. 1*C*) were dramatically increased in the follicular MGCs after mice were injected with 3-NP for 5 days. Under the same condition, although ROS signals in brain, liver, kidney, and spleen were detectable, no significant changes of ROS in these tissues were found compared with that from the negative control mice (Fig. 1*E*). Our results suggest the specificity of oxidant effects on the follicular MGCs rather than on other tested tissues in the 3-NP injection mouse model. Moreover, our qRT-PCR assay results showed that the mRNA levels of proapoptotic genes (*Bim*, *TRAIL*, and caspase-3) significantly increased in the 3-NP-treated MGCs (Fig. 1*D*). Considering the fact that 3-NP is able to induce oxidative stress and ATP reduction, both of which could potentially lead to apoptosis, the apoptosis observed in follicular MGCs following 3-NP treatment might not be caused fully by oxidative stress. Nevertheless, our data suggest that the 3-NP-treated mouse could be a relevant oxidative model for studying the oxidative stress and apoptosis conditions in follicular MGCs.

Oxidative Stress Affected FoxO Member Expressions in Follicular MGCs—FoxO mRNA levels were measured by qRT-PCR. When mice were treated with 3-NP, both FoxO1- and FoxO3-specific mRNA levels were significantly increased by 7.86- and 3.21-fold, respectively. However, no significant change in FoxO4 mRNA level was detected. The results indicate that oxidant 3-NP is able to induce FoxO1 and FoxO3 mRNA transcription in the follicular MGCs. Because the FoxO1 expression has a higher induced capability than that of FoxO3 in the 3-NP-treated follicular MGCs, we decided to mainly focus on FoxO1 function in this study. Consistent with the data from qRT-PCR

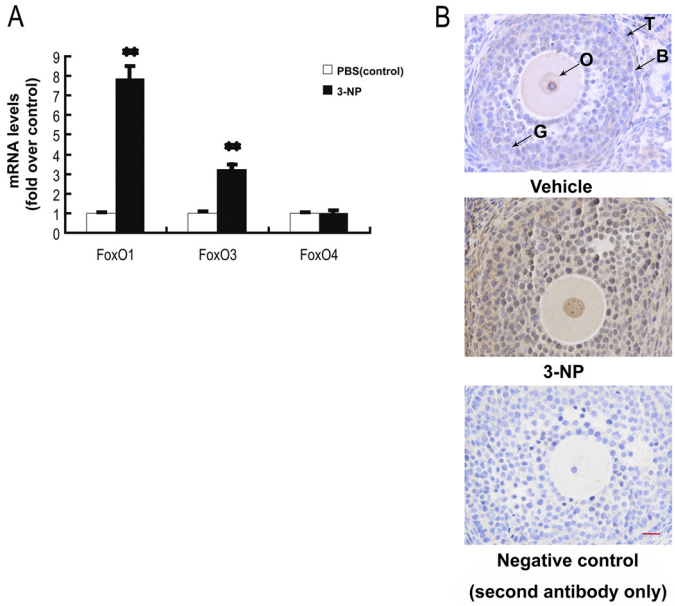

FIGURE 2. **Oxidative stress up-regulates FoxO1 expression in follicular MGCs.** *A*, qRT-PCR showed mRNA transcription changes of FoxO members in response to oxidative stress in follicular MGCs. Data are mean ± S.E. (*error bars*) ($n = 3$). The relative expression data were normalized to the amount of cellular β-actin. The statistical significance between groups was analyzed by one-way ANOVA. *, $p < 0.05$; **, $p < 0.01$. *B*, immunostaining of granulosa cells in ovary sections was detected by using anti-FoxO1 as described under "Experimental Procedures." *Bar*, 20 μm. *O*, oocyte; *G*, granulosa cells; *B*, basement membrane; *T*, theca cells.

assays, the FoxO1 protein levels were enhanced following 3-NP treatment (Fig. 2*B*), when the mouse ovary sections stained immunohistologically. In the injected mice, the 3-NP treatment consistently enhanced the expression of FoxO1 protein in follicular MGCs. The data imply a possible connection among oxidative stress, apoptosis, and FoxO1 expression in the 3-NP-treated follicular MGCs.

Oxidative Stress Induced Apoptosis in Cultured MGCs —To further confirm the effects of oxidative stress on follicular MGCs apoptosis and avoid possible ATP reduction from 3-NP treatment, we applied H_2O_2 treatment in primary cultured MGCs and pursued very similar approaches mentioned *in vivo* above. Fig. 3, *A* and *B*, shows the measurement of intracellular ROS induced by H_2O_2 treatment in the cultured MGCs. As assessed by dihydroethidium bromide fluorescence, the ROS-positive cells as well as the fluorescence levels are increased in a dose-dependent manner when exposed to H_2O_2 for 24 h. In Fig. 3*C*, the H_2O_2-treated cells displayed typical shrinkage and membrane bubbling as apoptosis characteristics. DAPI stained cells (*bottom*) also exhibited nuclear condensation and fragmentation in the oxidant-treated cells. To evaluate the effects of ROS accumulation on MGCs apoptosis, the cultured MGCs were treated with H_2O_2 in various concentrations as indicated for 24 h (Fig. 3*D*). The apoptotic effects detected by a TUNEL assay showed a dose-dependent increase in the number of apoptosis-positive MGCs after the H_2O_2 treatment (Fig. 3, *D* and *E*).

To avoid overoxidation that may cause non-physiological cell death, the minimal dose of H_2O_2 that generates substantial apoptosis was determined. Because cells treated with 100 μM H_2O_2 exhibited significantly higher apoptosis rates (Fig. 3, *D* and *E*) and cellular ROS levels (Fig. 3, *A* and *B*) than those treated with a negative control, the dose of 100 μM H_2O_2 was considered the minimal dose to trigger apoptosis in the cultured MGCs and was chosen for the subsequent experiments. Meanwhile, qRT-PCR was performed to examine transcript levels of several apoptotic genes, including *Bim*, *TRAIL*, *FasL*, and caspase-3. These mRNA expressions were remarkably enhanced in the cells treated with H_2O_2 for 24 h (Fig. 3*F*). Taken together, the results suggest that *in vitro* oxidative stress induced by H_2O_2 triggers apoptosis in cultured MGCs.

Oxidative Stress-dependent Induction of FoxO1 Expression in MGCs—Although previous studies suggest that FoxO activity is regulated by oxidative stress, those studies largely focused on the altered FoxO activity resulting from posttranslational modification and/or subcellular localization (39). It is not very clear whether oxidative stress exerts an effect on FoxO expression. An up-regulation of FoxO1 expression in follicular MGCs was detected in mice injected with 3-NP (Fig. 2*A*). To confirm the *in vivo* observation, the FoxO1 expression levels were evaluated in cultured MGCs treated with H_2O_2. As shown in Fig. 4, both FoxO1 mRNA and protein levels were significantly elevated in the H_2O_2-treated MGCs (Fig. 4, *A*–*C*). Taken together, the data from *in vivo* (Fig. 2) and *in vitro* models demonstrated that FoxO1 was up-regulated by the oxidant treatment in MGCs. In addition, immunofluorescence studies indicated that H_2O_2 treatment induced nuclear translocation of FoxO1 (Fig. 4*D* and supplemental Fig. S1), suggesting an increase of FoxO1 transactivation activity under the condition. All of these results are in line with the notion that H_2O_2 treatment is able to facilitate FoxO1 activity in MGCs.

Overexpression of FoxO1 Up-regulated the Expression of Pro-apoptotic Genes in MGCs—Because our data (Figs. 3 and 4) showed that H_2O_2 treatment induced FoxO1 activation and apoptosis in MGCs, the roles of FoxO1 in MGC apoptosis were investigated. We first determined the effects of overexpression of either wild-type FoxO1 or a constitutively active FoxO1 mutant on apoptosis in MGCs. As shown in Fig. 5*A*, Annexin V-propidium iodide (*PI*) staining indicated that cell apoptosis was increased significantly after transfection with wild-type FoxO1 expression vector. Fig. 5*B* showed FoxO1 nuclear translocation compared with a control group in MGCs, suggesting that enhanced FoxO1 expression might promote the nuclear FoxO1 translocation. This observation is consistent with the results obtained from the oxidant treatment test (Fig. 4*D* and supplemental Fig. S1). To further test if the overexpressed FoxO1 is related to inducing the MGC apoptosis, mRNA levels of apoptosis-related genes, *Bim*, *TRAIL*, *FasL*, and caspase-3, were measured by qRT-PCR. We found that all of the tested transcripts were significantly increased after overexpression of FoxO1 compared with levels in cells transfected with empty vector (Fig. 5*C*). The result suggests that overexpressed transcription factor FoxO1 activates its downstream apoptotic gene expression, thereby causing an enhancement of apoptosis in the MGCs.

Knockdown of FoxO1 Attenuated H_2O_2-induced Apoptosis in MGCs—We next determined whether FoxO1 played a major role in apoptosis of the oxidant-induced MGCs, in other words whether loss of FoxO1 function may prevent MGCs from such

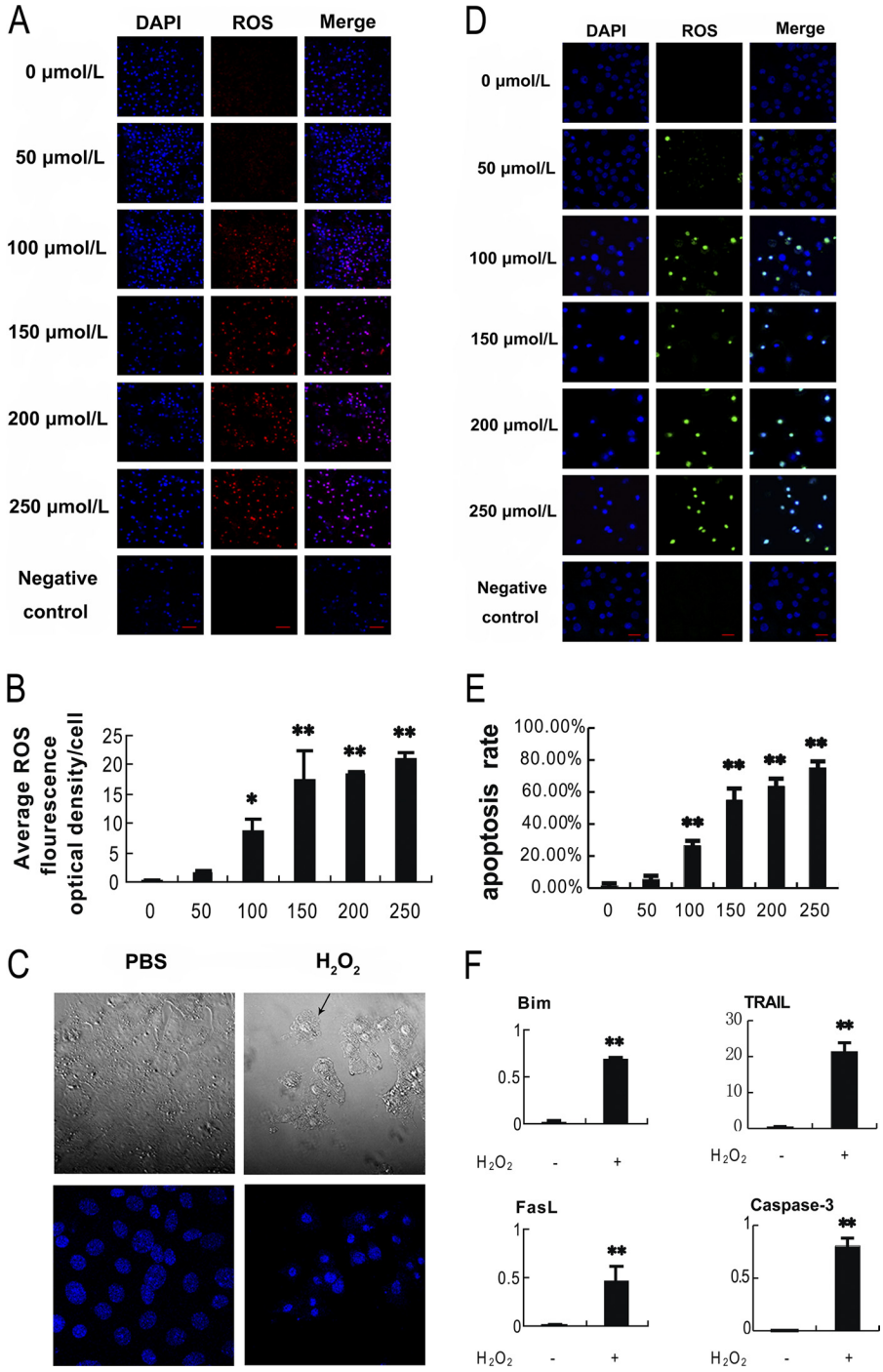

FIGURE 3. **Oxidative stress-induced apoptosis in cultured MGCs.** MGCs were treated with H_2O_2 at different concentrations as indicated for 24 h before harvested for tests. *A*, intracellular ROS were accumulated in a H_2O_2 dose-dependent manner. The ROS levels were detected by dihydroethidium bromide fluorescence (*red*), and nuclei were counterstained with DAPI (*blue*). *B*, quantification of intracellular ROS levels. ImageJ software was employed to analyze the optical density in each cell represented in *A*. *C*, H_2O_2 treatment induced apoptosis in MGCs. MGCs treated with or without H_2O_2 for 24 h were observed using laser confocal-scanning microscopy. *Bottom*, nuclei were stained with DAPI (*blue*). Magnification was ×400. *D*, apoptosis increased in a H_2O_2 dose-dependent manner in MGCs. Apoptosis was detected by TUNEL staining (FITC labeling). TUNEL-positive cells were displayed in green staining in the nuclei, which merged with the DAPI counterstaining (*blue*). *Bar*, 20 μm. *E*, quantification of the apoptosis rates (average number of TUNEL-positive staining nuclei per visual field). Experiments were repeated in triplicate, and three fields of each coverslip were selected in random for counting. Data represent mean ± S.E. (*error bars*) ($n = 3$). *F*, H_2O_2 promotes the expression of apoptosis relative genes. qRT-PCR was applied to detect the relative expression of these genes. The relative expression data were normalized to the amount of cellular β-actin. Data represent mean ± S.E. ($n = 3$). The statistical significance between groups was analyzed by one-way ANOVA. *, $p < 0.05$; **, $p < 0.01$.

programmed cellular death induced by oxidative stress. Plasmids expressing shRNAs were used to specifically knock down FoxO1 mRNA in the cultured MGCs, followed by treatment of the cells with H_2O_2. Four shRNAs against FoxO1 were first screened for their potency and specificity. shRNA 1979 was identified as the most potent and specific shRNA in silencing FoxO1 and was used for the subsequent experiments (Fig. 6*A*). After primary MGCs were transfected with FoxO1 shRNA

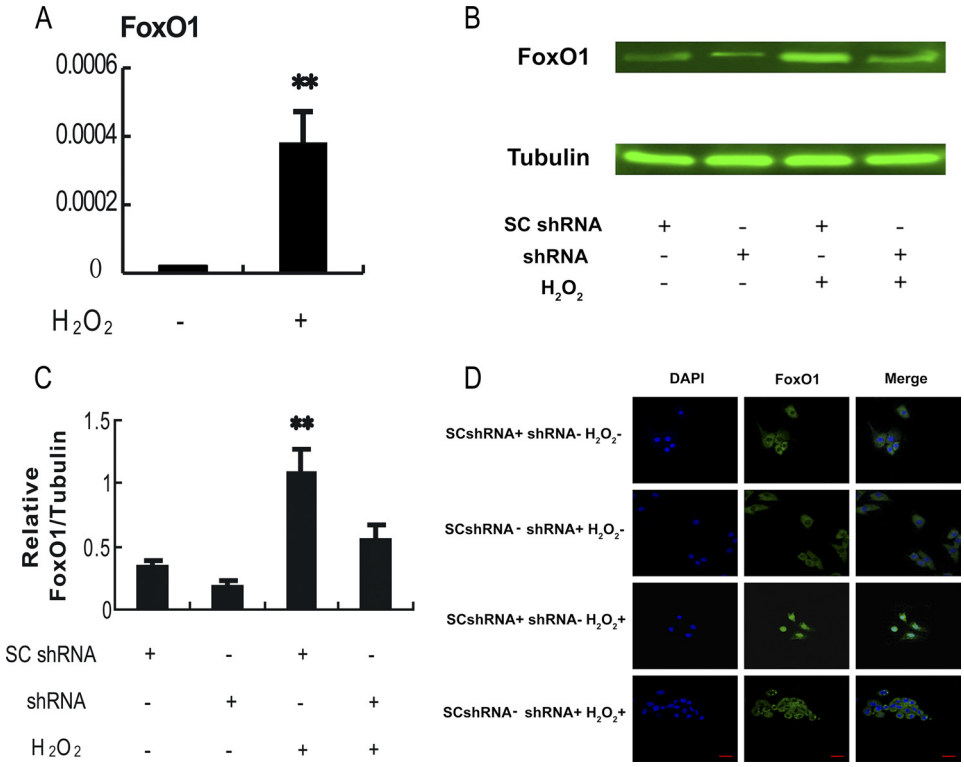

FIGURE 4. **Oxidative stress-dependent induction of FoxO1 in the cultured MGCs.** Primary MGCs were transfected with FoxO1 shRNA or control scramble shRNA (Fig. 6) for 24 h and exposed to 100 μM H_2O_2 for another 24 h before the cells were collected for tests. *A*, H_2O_2 treatment elevated FoxO1 mRNA expression in the cultured MGCs. Quantitative RT-PCR was employed to detect the relative expression of FoxO1. The expression data were normalized to the amount of cellular β-actin. *B*, H_2O_2 enhanced FoxO1 protein level in MGCs. Whole cell lysates were harvested from different treatment groups as indicated, and immunoblotting was performed to detect FoxO1 expression. α-Tubulin served as an internal control. *C*, quantification of relative FoxO1 protein level by gradation analyses. ImageJ software was applied to analyze the gradation of each band represented in Fig. 4*B*, and the relative expression level was normalized to the expression amount of α-tubulin. *D*, subcellular localization of FoxO1 in response to oxidative stress. Immunofluorescence of MGCs was imaged using anti-FoxO1 (*green*), and the nuclei were counterstained with DAPI (*blue*) (*bar*, 20 μm). The corresponding data above are represented as mean ± S.E. (*error bars*) ($n = 3$). The statistical significance between groups was analyzed by one-way ANOVA. *, $p < 0.05$; **, $p < 0.01$.

plasmid or scrambled control shRNA plasmid for 24 h, the cells were treated with 100 μM H_2O_2 for 24 h, followed by assay of FoxO1 expression, translocation, its target gene expression, and apoptosis. Data from the qRT-PCR assay showed that transfection of FoxO1 shRNA plasmid strikingly knocked down FoxO1 mRNA level, which was elevated by H_2O_2 treatment (Fig. 6*B*). In agreement with this observation, transfection of FoxO1 shRNA plasmid also reduced FoxO1 protein levels in the MGCs treated with or without H_2O_2 (Fig. 4*B*). Immunofluorescence from FoxO1 antibody indicated that transfecting FoxO1 shRNA abolished the nuclear distribution of FoxO1 in MGCs (Fig. 4*D* and supplemental Fig. S1).

We next evaluated the effects of FoxO1 on apoptosis under the same oxidative stress condition. It was found that TUNEL-positive signals were significantly abrogated in the FoxO1 shRNA transfection group (Fig. 6, *C* and *D*). Furthermore, the mRNA levels of apoptosis-related genes (*Bim*, *TRAIL*, *FasL*, and caspase-3) were significantly reduced as a result of FoxO1 knockdown (Fig. 6*E*). The results suggest that knockdown of FoxO1 attenuates the transcriptional activation of its downstream target genes involved in apoptotic process, and therefore protecting MGCs from the H_2O_2-induced apoptosis. Thus, it was concluded that FoxO1 plays a pivotal role in the oxidant-induced apoptosis in MGCs.

Insulin Inhibits H_2O_2-induced Apoptosis in MGCs—Previous studies have shown that FoxO1 activity is repressed by insulin, which induces FoxO1 phosphorylation through activation of the PKB/AKT signaling pathway, and therefore preventing FoxO1 from entering into the cell nucleus (51). To further confirm the role of FoxO1 in MGC apoptosis, we applied insulin treatment in our MGC model. MGCs were treated with 100 ng/ml insulin for 24 h, followed by treatment with 100 μM H_2O_2 for another 24 h. As shown in Fig. 7*A*, when insulin was absent, the oxidant H_2O_2 treatment enhanced FoxO1 nuclear translocation. In contrast, the presence of insulin attenuated FoxO1 nucleus localization strikingly (Fig. 7*A* and supplemental Fig. S4). The result indicated that the phosphorylated FoxO1 proteins remained in the cytosol. Also, TUNEL data showed that DNA fragmentation in the H_2O_2-treated MGCs decreased significantly when the cells were treated with insulin (Fig. 7, *B* and *C*). The result implied that insulin treatment reduced H_2O_2-induced apoptosis. As expected from the MGCs, our qRT-PCR data shown in Fig. 7*D* confirmed that H_2O_2 treatment failed to induce mRNA levels of apoptosis-related genes, *Bim*, *TRAIL*, *FasL*, and caspase-3, when the MGCs were treated with insulin. All of these data are in line with the notion that insulin inhibits the nuclear translocation of FoxO1 induced by the oxidant treatment, consequently repressing the expression of the FoxO1 target apoptosis-related genes and reducing the apoptosis rate in MGCs. It appears that as a transcriptional activator, FoxO1 exerts its activity in cell nucleus and plays a major role in MGC apoptosis during the oxidative stimulation.

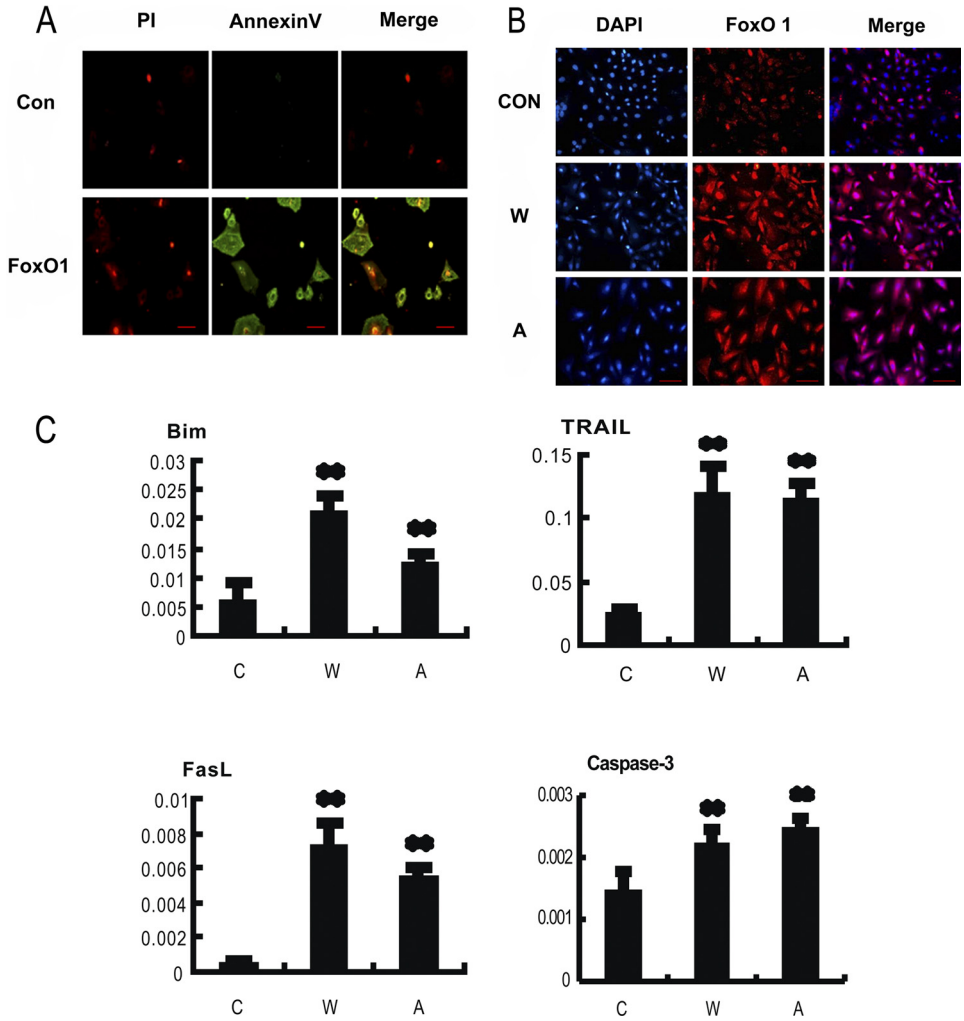

FIGURE 5. **Overexpression of FoxO1 induces apoptosis in MGCs.** MGCs were transfected with plasmids encoding wild-type FoxO1 (*W*), a constitutively active FoxO1 mutant (*A*), and a non-transfection control (*C*), respectively. *A*, overexpression of FoxO1 (*W*) promoted apoptosis in cultured MGCs. Apoptosis images were visualized with propidium iodide/annexin V-FITC staining (*bar*, 100 μm). *B*, overexpression of FoxO1 induced a nuclear accumulation of FoxO1 protein. Immunofluorescence was performed using anti-FoxO1 (*red*), and the nuclei were counterstained with DAPI (*blue*). *Bar*, 100 μm. *C*, overexpression of FoxO1 increased mRNA levels of apoptosis-related genes. Quantitative RT-PCR was applied to measure the corresponding mRNA levels. The relative expression data were normalized to the amount of cellular β-actin. The corresponding data above represent mean $\pm$ S.E. (*error bars*) ($n = 3$). The statistical significance between groups was analyzed by one-way ANOVA. *, $p < 0.05$; **, $p < 0.01$.

DISCUSSION

In this study, we provided new insights into the regulation of apoptosis in response to oxidative stress in granulosa cells. Oxidant 3-NP was used to generate oxidative stress on ovaries in a mouse model, in which ROS specifically increased in follicular granulosa cells but not other tissues we examined (Fig. 1). Also, when using 3-NP to inject mice or H_2O_2 to treat primary cultured MGCs, it was found that FoxO1 expression was dramatically up-regulated in the oxidative stress condition, followed by elevation of the apoptosis-related gene expressions as well as an increase of cell apoptosis in MGCs (Figs. 1–4). Overexpression of wild-type FoxO1 or a constitutively active FoxO1 mutant apparently enhanced MGC apoptosis rates (Fig. 5). In contrast, when the FoxO1 expression is knocking down, the MGCs could be prevented from the oxidant-induced apoptosis (Fig. 6). Moreover, our results showed that the insulin treatment inhibited FoxO1 nuclear translocation, consistent with reports from other research groups that inhibition of FoxO1 translocation reduces apoptosis-related gene expression and prevents cell apoptosis in the MGCs treated with oxidant H_2O_2 (Fig. 7). Thus, evidence strongly suggests that FoxO1 plays a pivotal role in oxidative stress-induced MGC apoptosis, which can be inhibited by other preventive signaling.

Evidence from various types of mammal cells indicates that FoxO1 induces apoptosis by activating apoptosis-related gene expression (64). In fact, several FoxO1 target proapoptotic genes have been identified (44, 45, 51, 65, 66). For example, three conservative FoxO member-binding sites are located within the promoter of *FasL* in CHO cells and human 293T cells (51). *FasL* is a proapoptotic gene encoding a protein specifically combining with the death receptor APO-1/CD95 and activates apoptosis in human cells (67). Similarly, FoxO1 induces the expression of *TRAIL* in human prostate cancer cells because the *TRAIL* promoter contains a FoxO consensus site, indicating that *TRAIL* is a direct target of FoxO1 (45). TRAIL as a death receptor ligand promotes apoptosis via a death receptor

signaling pathway (67). Also, FoxO1 is involved in transactivating the expression of *Bim*, which encodes a BH3-only protein belonging to the Bcl-2 family and triggers apoptosis in a mitochondria-dependent pathway. It has been found that two FoxO consensus sites exist in the promoter region of *Bim* in rat cells (44). In this study, it was found that *Bim*, *TRAIL*, and *FasL* expression was up-regulated in a FoxO1-dependent manner in the mouse granulosa cells either treated *in vivo* with oxidant 3-NP (Fig. 1*D*) or treated *in vitro* with H_2O_2 (Fig. 3*F*). Interestingly, when we specifically attenuated endogenous FoxO1 expression in mouse granulosa cells by RNAi, the expression of proapoptotic genes, *Bim*, *TRAIL*, and *FasL*, was subsequently

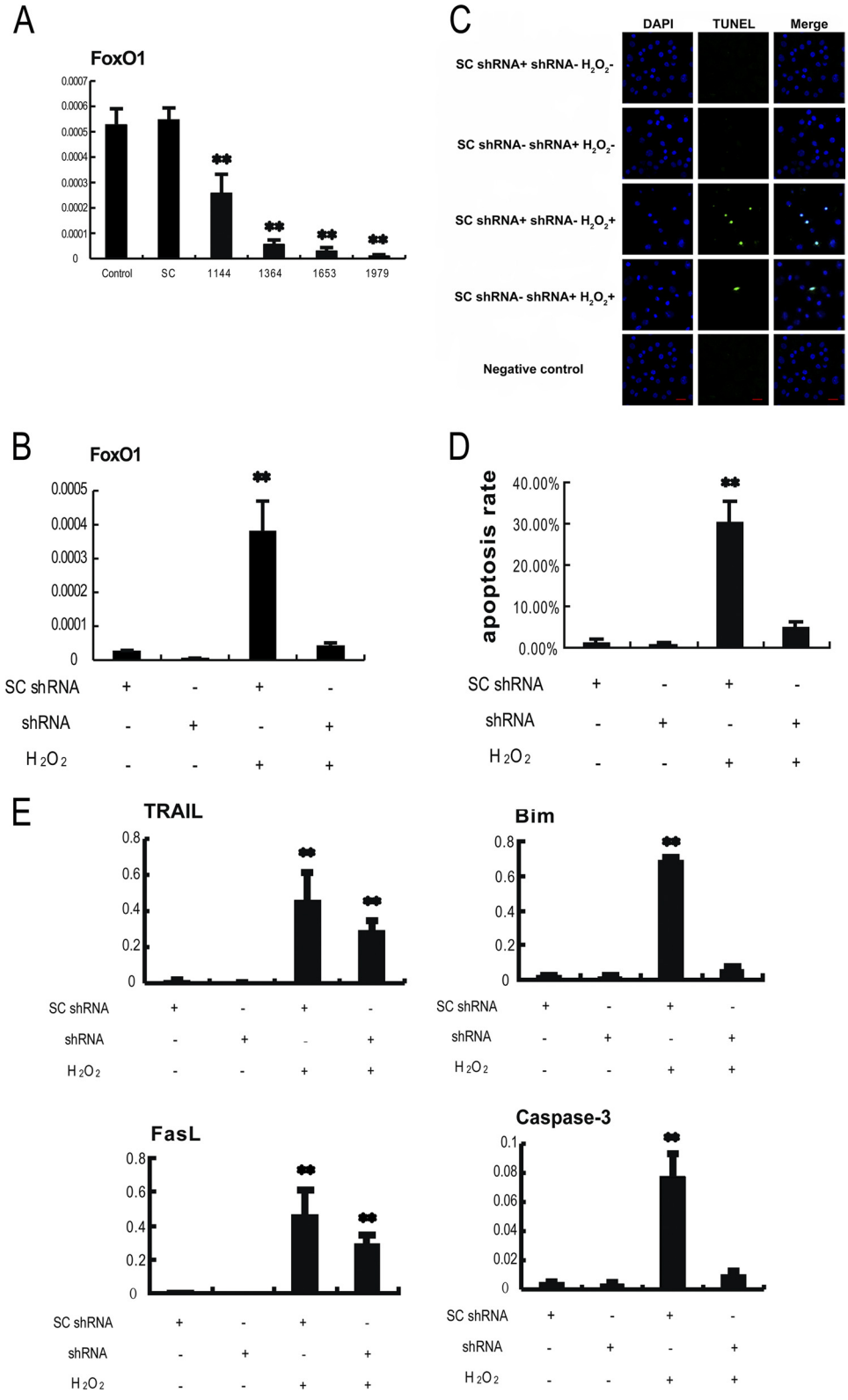

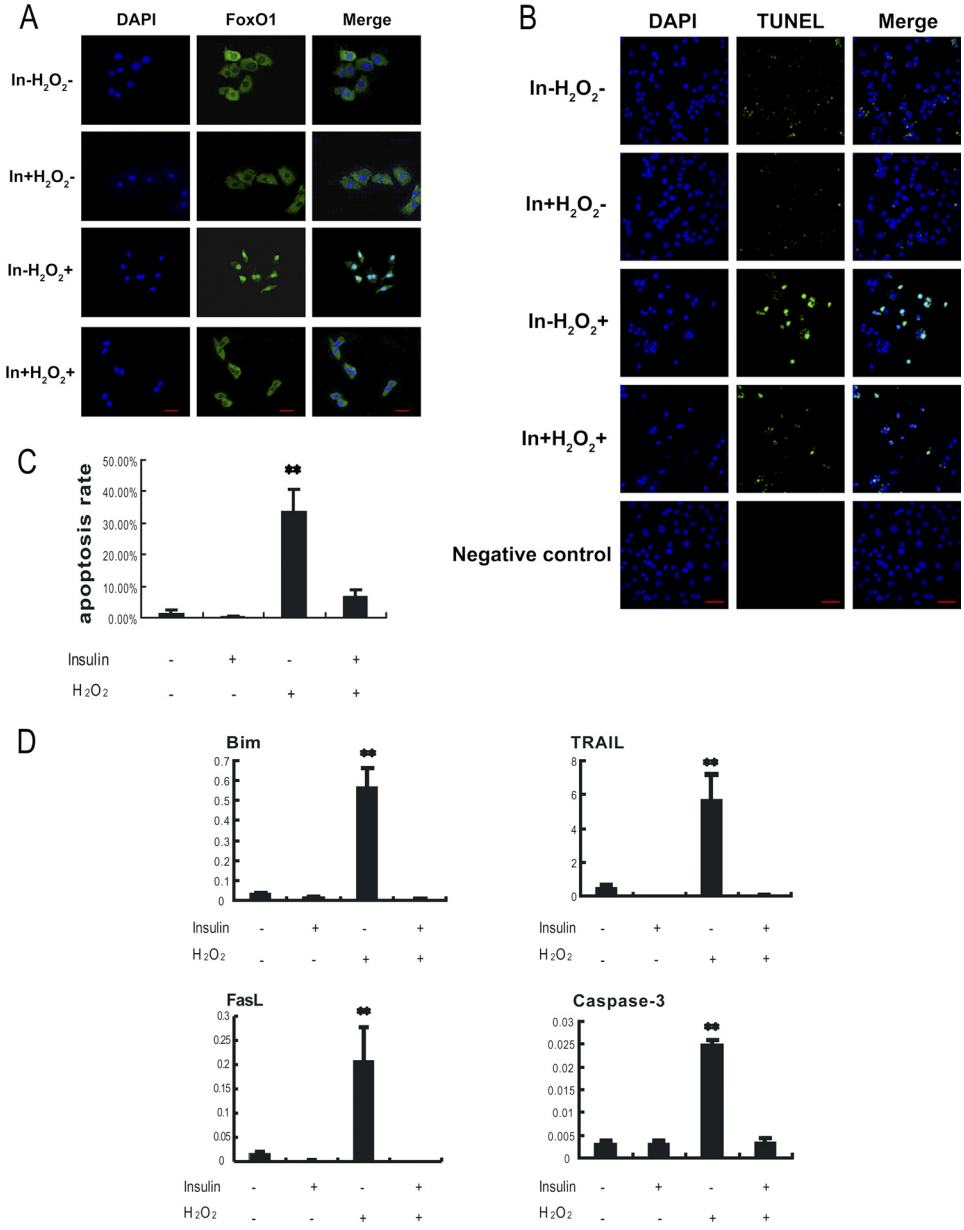

FIGURE 7. **Insulin inhibited H_2O_2 induced apoptosis in MGCs.** Primary cultured MGCs were treated with 100 ng/ml insulin for 24 h and exposed to 100 μM H_2O_2 for another 24 h. *A*, immunofluorescence subcellular localization of FoxO1 under insulin treatment was performed using anti-FoxO1 (*green*), and the nuclei were counterstained with DAPI (*blue*). *Bar*, 20 μm. *B*, insulin decreased apoptosis in MGCs. Apoptosis was detected by a TUNEL assay (FITC labeling). TUNEL-positive cells displayed *green* staining in the nuclei, which was merged with the DAPI counterstaining (*blue*). *Bar*, 50 μm. *C*, the TUNEL-positive rates were determined by averaging numbers of TUNEL-positive staining nuclei from three randomly chosen visual fields in each coverslip. Experiments were repeated in triplicate. *D*, insulin attenuated the expression of apoptosis-related genes. Quantitative RT-PCR was performed to measure mRNA levels of genes interested. The relative expression levels were normalized to the expression amount of β-actin. Data are mean $\pm$ S.E. (*error bars*) ($n = 3$). The statistical significance between groups was analyzed by one-way ANOVA. *, $p < 0.05$; **, $p < 0.01$.

FIGURE 6. **Knocking down FoxO1 with shRNA inhibits H_2O_2-induced apoptosis in MGCs.** *A*, the screening of the most effective FoxO1 shRNA. Primary cultures of MGCs remained as an untreated control or were transfected with FoxO1 shRNAs targeting different sites of FoxO1 mRNA (1144, 1364, 1653, and 1979) or scramble control shRNA (*SC*) for 24 h. The cultures were collected for a quantitative RT-PCR assay, and the relative expression levels were normalized to the expression amount of β-actin. *B–E*, primary MGCs were transfected with FoxO1 shRNA or scramble shRNA for 24 h and exposed to 100 μM H_2O_2 for another 24 h. The cells were harvested for a TUNEL assay or qRT-PCR. *B*, quantitative RT-PCR showing relative expression of FoxO1. *C*, knocking down FoxO1 decreased apoptosis in MGCs. Apoptotic images were visualized by a TUNEL assay. TUNEL-positive cells display green staining in the nuclei, which merged with the DAPI counterstaining (*blue*). *Bar*, 20 μm. *D*, the TUNEL-positive rates were determined by averaging numbers of TUNEL-positive staining nuclei from three randomly chosen visual fields in each coverslip. Experiments were repeated in triplicate. *E*, knocking down FoxO1 attenuated the expression of apoptosis-related genes. Quantitative RT-PCR was performed to measure the mRNA levels. The relative expression levels were normalized to the expression amount of β-actin. The corresponding data above represent mean $\pm$ S.E. (*error bars*) ($n = 3$). The statistical significance between groups was analyzed by one-way ANOVA. *, $p < 0.05$; **, $p < 0.01$.

reduced (Fig. 6*E*). In fact, the overexpression of a wild-type FoxO1 or a constitutively active mutant FoxO1 induced a significant increase of mRNA levels of these proapoptotic genes (Fig. 5*C*). Our data suggest that the proapoptotic genes, *Bim*, *TRAIL*, and *FasL*, their expressions being up-regulated by the FoxO1 activation in MGCs, may be similar to the genes previously reported in the other mammal cells.

Cell apoptosis can be initiated by a mitochondria-dependent or -independent apoptosis pathway (68). Both pathways trigger apoptosis by activating different caspase cascades and converging on caspase-3, the executor of apoptosis. In our study, the caspase-3 mRNA level increased with oxidant treatment or FoxO1 overexpression in MGCs, which is positively correlated with elevating expression of *Bim*, *TRAIL*, and *FasL* (Figs. 1*D*, 3*F*, and 5*C*). Although it was not known whether FoxO1 directly transactivated caspase-3, the elevation of caspase-3 expression by FoxO1 up-regulation suggested that caspase-3 could act in concert with *Bim*, *TRAIL*, and *FasL* in oxidative stress-induced MGC apoptosis.

Moreover, we inhibited FoxO1 activity by insulin in primary cultured MGCs (Fig. 7). This result suggested that FoxO1 is a player in the induction of MGCs apoptosis under oxidative conditions. FoxO members have consensus Akt phosphorylation sites in the Forkhead domains (39). Through the insulin signaling pathway, Akt phosphorylates FoxO members at these sites, facilitating their binding to 14-3-3 proteins, and the subsequent sequestration in the cytoplasm, thus promotes cell survival (51).

Akt activity is regulated cell type-dependently. For example, NADPH oxidase 2-derived oxidative stress down-regulates AKT activity in pancreatic β-cells, resulting in FoxO1 nuclear translocation and apoptosis (69). However, in vascular endothelial cells, kallistatin attenuates apoptosis during oxidative stress by activating Akt signaling and down-regulating FoxO1 expression (70). Therefore, we evaluated the phosphorylation levels of serine 256 and 319 residues in FoxO1. However, we observed a possible change of less phosphorylation in these sites under oxidative stress in MGCs (supplemental Fig. S2). It could be interpreted that Akt signaling may not be active in the oxidative stress-induced apoptosis; nevertheless, this situation favored MGC apoptosis under oxidative conditions.

In addition to triggering apoptosis, FoxO members also play a role in stress resistance and protect cells from oxidative damage. In *Caenorhabditis elegans*, oxidative stress can induce DAF-16 (a homologue of mammalian FoxO)-dependent expression of catalase and SOD3 (a homologue of mammalian Mn-SOD) and prolong the life span of *C. elegans* (46). In quiescent cells, FoxO3 activated by oxidative stress can enhance the expression of Mn-SOD and protect cells from oxidative damage (53). In addition, inhibition of FoxO activity by PKB/Akt reduces the expression of Mn-SOD and catalase (53, 71). Expression of FoxO3 results in an increase in catalase expression levels in human cells (71). Moreover, conserved FoxO binding sites are located within the promoter of glutathione peroxidase in both mice and humans, implying that glutathione peroxidase is a direct target of FoxO (54). In our study, up-regulation of FoxO1 expression was associated with substantial elevation of Mn-SOD, catalase, and glutathione peroxidase expression in MGCs under oxidative stress (supplemental Fig. S5). Our data agreed with previous observations in other cell types (39). Thus, under oxidative stress conditions, FoxO1 can either trigger apoptosis by inducing proapoptotic genes or promote cell survival by up-regulating antioxidant genes. These observations support the notion that cell fate in response to oxidative stress is dependent upon cell type, cell differentiating state, or oxidant treatment conditions (6). A summary shown in Fig. 8 displays a mechanism by which FoxO1 (or other FoxO members) may act as a sensor in modulating the fate of cell apoptosis under oxidative stress.

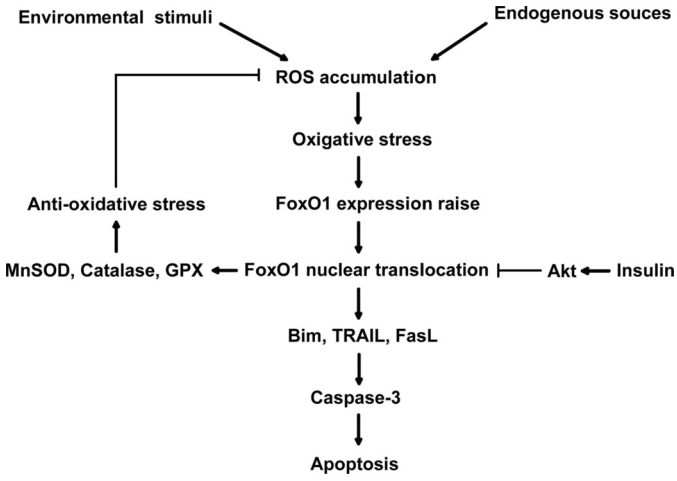

FIGURE 8. **A model of the role of FoxO1 in oxidative stress-induced apoptosis in mouse granulosa cells.** When ROS is generated either by endogenous sources like aerobic metabolism and ischemia or by environmental stress like ionizing radiation and UV light, the excessive ROS accumulation results in oxidative stress in the cells. As a pivotal sensor of intracellular ROS, FoxO1 function is enhanced by both FoxO1 expression up-regulation and nuclear translocation, therefore activating the transcription of FoxO1 target genes, including either proapoptosis or stress-resistant genes. The proapoptotic genes transfer the stress signal through mitochondrial pathway and finally initiate caspase-3 activity and cell apoptosis. But the oxidative stress-resistant genes serve to reduce the cellular ROS level, which may provide negative feedback to balance the FoxO1 expression during oxidative stress. Independently, insulin signaling can reduce the FoxO1 function via the PKB/AKT pathway phosphorylating FoxO1 and prohibiting the FoxO1 nuclear localization, thereby protecting granulosa cells from oxidative stress-induced apoptosis.

Although there are many oxidative stress models, few have been well applied for the follicular atresia studies. It has been reported that oxidative stress derived from the *in vivo* treatment of methoxychlor can inhibit follicular growth and lead to follicular atresia in the mouse ovary (21). As an organochlorine pesticide, methoxychlor causes damages in liver, kidney, and cardiac cells due to its toxic effects (72). 4-Vinylcyclohexene was also reported as a toxin targeting mouse ovaries, but 4-vinylcyclohexene-induced follicle loss is not related to oxidative stress (73, 74). Oxidative stress has been reported when rodent models were treated with 3-NP (27–30). For example, a high ROS level was detected in rat striatum intraperitoneally injected with 3-NP, and this effect was attenuated by free radical scavengers, antioxidants, and NO synthase inhibitor (28). Another report indicated that free radicals play a role in neuronal damage induced by 3-NP in injected rats (27). 3-NP has been used in mammal models simulating neurodegenerative diseases (26). However, there is little evidence of oxidative stress effects on follicular atresia in rodent models. In this study, we used 3-NP to establish a mouse model for simulating

oxidative stress specified in mammal ovaries. According to our treatment procedure, we succeeded in inducing oxidative stress in follicles when the mice were injected with 3-NP, increasing ROS levels in follicular MGCs (Fig. 1, *A* and *B*). Exclusively, ROS levels in brain, liver, kidney, and spleen remained constant in the 3-NP-injected mice (Fig. 1*E*). From our ongoing experiments, our data[4] showed that 1) no significant difference in the mouse growth rate between the 3-NP-treated and untreated groups was detected; 2) no significant difference in mortality rate between the 3-NP-treated and untreated groups was observed; 3) the ovary weight was reduced significantly in the 3-NP-treated group compared with the untreated group, whereas the weights of other tissues (brain, kidney, liver, and spleen) were similar in both groups; and 4) the ratio of *Bcl-2*/*Bax* mRNA (indicating apoptotic effect) was significantly increased in the follicular MGCs after mice were injected with 3-NP compared with the control group, whereas such ratios in other tissues (brain, kidney, liver, and spleen) were similar in both groups. These observations indicated the specificity of oxidative stress effects on MGCs under 3-NP treatment conditions. Using our 3-NP-treated mouse model, we cannot explain why ROS levels were not boosted in the brain, although a previous study reported that 3-NP could induce oxidative stress in the stratum and cortex (28). The difference may be due to different rodent species, mouse breeding, and/or raising environments.

In our another ongoing experiment to confirm the effect of 3-NP on follicular atresia, we found that the ovaries from mice injected with 3-NP had fewer follicles and that their follicular fluid looked opaque compared with that of untreated controls (data not shown). Our data[4] also showed that the 3-NP treatment reduced large follicle numbers and increased follicular atresia in the mouse ovary. These results were consistent with previous reports of oxidative stress-induced follicular atresia in other oxidant-treated mammals (14–16). Hence, the 3-NP treatment mouse model may be eligible as an experimental oxidative stress platform to evaluate the effects of antioxidants on the development of mammal ovaries in future studies.

Because granulosa cell apoptosis is the main marker of follicular atresia (75), establishing oxidative models specific to ovary follicular granulosa cells will be useful in the study of follicular atresia. H_2O_2 is commonly used to produce oxidative stress in cultured cells (31, 34). However, few reports described applying H_2O_2 to research oxidative stress in granulosa cells. In this study, H_2O_2-treated primary MGCs was used as an oxidative stress model, in which ROS levels and apoptosis rate increased in MGCs in an H_2O_2 dose-dependent manner. Importantly, the FoxO1 expression was dramatically up-regulated under the same conditions. Moreover, we proved that oxidative stress-induced FoxO1 expression caused cell apoptosis. Thus, the *in vitro* model allowed us to manipulate the expression of FoxO1 to elucidate the mechanism involved in oxidative stress-induced apoptosis in MGCs.

Obviously, there are other stress types in addition to oxidative stress, such as heat stress, cold stress, and starvation stress. Many studies suggest that there is a link among these various stresses in animals. For example, heat stress is implicated to generate ROS, because the gene expression pattern induced by heat stress (heat shock protein and oxidative response protein) is similar to that triggered by oxidative stress (76–77). The ROS derived from heat stress is considered to be responsible for the physiological dysfunction and the decline in animal performance (78). Cold stress can be simulated by keeping homeothermic animals in a cold environment. In response to the cold exposure, animals need a continuous supply of heat production to maintain body temperature (79). Oxidative stress has been detected in several animal tissues, which appears to be associated with the thyroid hormone level during cold stress (80). In addition to heat and cold stresses, starvation stress, restraint stress, psychological stress, and sleep deprivation stress are also proven to induce oxidative stress in the subject animals (81–83). Because these stresses are associated with oxidative stress, they may also be contributing factors that cause follicular atresia in mammals. Therefore, the study of the oxidative stress in MGCs will provide the potential to develop a relevant model to investigate the mechanisms associated with these stresses in the future.

[4] J. Zhang, C. Zhu, M. Shen, and H. Liu, unpublished data.

REFERENCES

1. Asselin, E., Xiao, C. W., Wang, Y. F., and Tsang, B. K. (2000) Mammalian follicular development and atresia. Role of apoptosis. *Biol. Signals Recept.* **9,** 87–95
2. Jiang, J. Y., Cheung, C. K., Wang, Y., and Tsang, B. K. (2003) Regulation of cell death and cell survival gene expression during ovarian follicular development and atresia. *Front. Biosci.* **8,** d222–d237
3. Valdez, K. E., Cuneo, S. P., and Turzillo, A. M. (2005) Regulation of apoptosis in the atresia of dominant bovine follicles of the first follicular wave following ovulation. *Reproduction* **130,** 71–81
4. Inoue, N., Maeda, A., Matsuda-Minehata, F., Fukuta, K., and Manabe, N. (2006) Expression and localization of Fas ligand and Fas during atresia in porcine ovarian follicles. *J. Reprod. Dev.* **52,** 723–730
5. Essers, M. A., Weijzen, S., de Vries-Smits, A. M., Saarloos, I., de Ruiter, N. D., Bos, J. L., and Burgering, B. M. (2004) FOXO transcription factor activation by oxidative stress mediated by the small GTPase Ral and JNK. *EMBO J.* **23,** 4802–4812
6. Storz, P. (2011) Forkhead homeobox type O transcription factors in the responses to oxidative stress. *Antioxid. Redox Signal.* **14,** 593–605
7. Essers, M. A., de Vries-Smits, L. M., Barker, N., Polderman, P. E., Burgering, B. M., and Korswagen, H. C. (2005) Functional interaction between β-catenin and FOXO in oxidative stress signaling. *Science* **308,** 1181–1184
8. Clopton, D. A., and Saltman, P. (1995) Low-level oxidative stress causes cell-cycle specific arrest in cultured cells. *Biochem. Biophys. Res. Commun.* **210,** 189–196
9. Dröge, W., and Kinscherf, R. (2008) Aberrant insulin receptor signaling and amino acid homeostasis as a major cause of oxidative stress in aging. *Antioxid. Redox Signal.* **10,** 661–678
10. Finkel, T., and Holbrook, N. J. (2000) Oxidants, oxidative stress and the biology of aging. *Nature* **408,** 239–247
11. Yang, J., Liu, X., Bhalla, K., Kim, C. N., Ibrado, A. M., Cai, J., Peng, T. I., Jones, D. P., and Wang, X. (1997) Prevention of apoptosis by Bcl-2. Release of cytochrome *c* from mitochondria blocked. *Science* **275,** 1129–1132
12. Franco, R., Sánchez-Olea, R., Reyes-Reyes, E. M., and Panayiotidis, M. I. (2009) Environmental toxicity, oxidative stress, and apoptosis. Menage a trois. *Mutat. Res.* **674,** 3–22
13. Murdoch, W. J. (1998) Inhibition by oestradiol of oxidative stress-induced apoptosis in pig ovarian tissues. *J. Reprod. Fertil.* **114,** 127–130
14. Kumar, M., Pathak, D., Kriplani, A., Ammini, A. C., Talwar, P., and Dada, R. (2010) Nucleotide variations in mitochondrial DNA and supraphysiological ROS levels in cytogenetically normal cases of premature ovarian

insufficiency. *Arch. Gynecol. Obstet.* **282,** 695–705
15. Ortega-Camarillo, C., González-González, A., Vergara-Onofre, M., González-Padilla, E., Avalos-Rodríguez, A., Gutiérrez-Rodríguez, M. E., Arriaga-Pizano, L., Cruz, M., Baiza-Gutman, L. A., and Díaz-Flores, M. (2009) Changes in the glucose-6-phosphate dehydrogenase activity in granulosa cells during follicular atresia in ewes. *Reproduction.* **137,** 979–986
16. Tilly, J. L., and Tilly, K. I. (1995) Inhibitors of oxidative stress mimic the ability of follicle-stimulating hormone to suppress apoptosis in cultured rat ovarian follicles. *Endocrinology* **136,** 242–252
17. Melov, S. (2002) Animal models of oxidative stress, aging, and therapeutic antioxidant interventions. *Int. J. Biochem. Cell Biol.* **34,** 1395–1400
18. Gille, J. J., and Joenje, H. (1992) Cell culture models for oxidative stress. Superoxide and hydrogen peroxide *versus* normobaric hyperoxia. *Mutat. Res.* **275,** 405–414
19. Song, X., Bao, M., Li, D., and Li, Y. M. (1999) Advanced glycation in D-galactose-induced mouse aging model. *Mech. Ageing Dev.* **108,** 239–251
20. Sener, G., Sehirli, O., Ipçi, Y., Cetinel, S., Cikler, E., Gedik, N., and Alican, I. (2005) Protective effects of taurine against nicotine-induced oxidative damage of rat urinary bladder and kidney. *Pharmacology* **74,** 37–44
21. Gupta, R. K., Meachum, S., Hernández-Ochoa, I., Peretz, J., Yao, H. H., and Flaws, J. A. (2009) Methoxychlor inhibits growth of antral follicles by altering cell cycle regulators. *Toxicol. Appl. Pharmacol.* **240,** 1–7
22. Alston, T. A., Mela, L., and Bright, H. J. (1977) 3-Nitropropionate, the toxic substance of Indigofera, is a suicide inactivator of succinate dehydrogenase. *Proc. Natl. Acad. Sci. U.S.A.* **74,** 3767–3771
23. Beal, M. F., Brouillet, E., Jenkins, B., Henshaw, R., Rosen, B., and Hyman, B. T. (1993) Age-dependent striatal excitotoxic lesions produced by the endogenous mitochondrial inhibitor malonate. *J. Neurochem.* **61,** 1147–1150
24. Brouillet, E., Hantraye, P., Ferrante, R. J., Dolan, R., Leroy-Willig, A., Kowall, N. W., and Beal, M. F. (1995) Chronic mitochondrial energy impairment produces selective striatal degeneration and abnormal choreiform movements in primates. *Proc. Natl. Acad. Sci. U.S.A.* **92,** 7105–7109
25. Montilla, P., Túnez, I., Muñoz, M. C., Salcedo, M., Feijóo, M., Muñoz-Castañeda, J. R., and Bujalance, I. (2004) Effect of glucocorticoids on 3-nitropropionic acid-induced oxidative stress in synaptosomes. *Eur. J. Pharmacol.* **488,** 19–25
26. Alexi, T., Hughes, P. E., Faull, R. L., and Williams, C. E. (1998) 3-Nitropropionic acid's lethal triplet. Cooperative pathways of neurodegeneration. *Neuroreport* **9,** R57–R64
27. Schulz, J. B., Henshaw, D. R., MacGarvey, U., and Beal, M. F. (1996) Involvement of oxidative stress in 3-nitropropionic acid neurotoxicity. *Neurochem. Int.* **29,** 167–171
28. Fontaine, M. A., Geddes, J. W., Banks, A., and Butterfield, D. A. (2000) Effect of exogenous and endogenous antioxidants on 3-nitropionic acid-induced *in vivo* oxidative stress and striatal lesions. Insights into Huntington's disease. *J. Neurochem.* **75,** 1709–1715
29. Kim, G. W., Copin, J. C., Kawase, M., Chen, S. F., Sato, S., Gobbel, G. T., and Chan, P. H. (2000) Excitotoxicity is required for induction of oxidative stress and apoptosis in mouse striatum by the mitochondrial toxin, 3-nitropropionic acid. *J. Cereb. Blood Flow Metab.* **20,** 119–129
30. Kumar, P., Kalonia, H., and Kumar, A. (2011) Novel protective mechanisms of antidepressants against 3-nitropropionic acid induced Huntington's-like symptoms. A comparative study. *J. Psychopharmacol.* **25,** 1399–1411
31. Kaczara, P., Sarna, T., and Burke, J. M. (2010) Dynamics of H_2O_2 availability to ARPE-19 cultures in models of oxidative stress. *Free Radic. Biol. Med.* **48,** 1064–1070
32. Henzler, T., and Steudle, E. (2000) Transport and metabolic degradation of hydrogen peroxide in *Chara corallina*. Model calculations and measurements with the pressure probe suggest transport of H_2O_2 across water channels. *J. Exp. Bot.* **51,** 2053–2066
33. Floyd, R. A., and Carney, J. M. (1992) Free radical damage to protein and DNA. Mechanisms involved and relevant observations on brain undergoing oxidative stress. *Ann. Neurol.* **32,** S22–S27
34. Farombi, E. O., Møller, P., and Dragsted, L. O. (2004) *Ex vivo* and *in vitro* protective effects of kolaviron against oxygen-derived radical-induced DNA damage and oxidative stress in human lymphocytes and rat liver cells. *Cell Biol. Toxicol.* **20,** 71–82
35. Barthel, A., Schmoll, D., and Unterman, T. G. (2005) FoxO proteins in insulin action and metabolism. *Trends Endocrinol. Metab.* **16,** 183–189
36. Accili, D., and Arden, K. C. (2004) FoxOs at the crossroads of cellular metabolism, differentiation, and transformation. *Cell* **117,** 421–426
37. Greer, E. L., and Brunet, A. (2005) FOXO transcription factors at the interface between longevity and tumor suppression. *Oncogene* **24,** 7410–7425
38. Giannakou, M. E., and Partridge, L. (2004) The interaction between FOXO and SIRT1. Tipping the balance towards survival. *Trends Cell Biol.* **14,** 408–412
39. Huang, H., and Tindall, D. J. (2007) Dynamic FoxO transcription factors. *J. Cell Sci.* **120,** 2479–2487
40. Hughes, K. J., Meares, G. P., Hansen, P. A., and Corbett, J. A. (2011) FoxO1 and SIRT1 regulate β-cell responses to nitric oxide. *J. Biol. Chem.* **286,** 8338–8348
41. Brunet, A., Kanai, F., Stehn, J., Xu, J., Sarbassova, D., Frangioni, J. V., Dalal, S. N., DeCaprio, J. A., Greenberg, M. E., and Yaffe, M. B. (2002) 14-3-3 transits to the nucleus and participates in dynamic nucleocytoplasmic transport. *J. Cell Biol.* **156,** 817–828
42. Nakamura, N., Ramaswamy, S., Vazquez, F., Signoretti, S., Loda, M., and Sellers, W. R. (2000) Forkhead transcription factors are critical effectors of cell death and cell cycle arrest downstream of PTEN. *Mol. Cell. Biol.* **20,** 8969–8982
43. Dijkers, P. F., Medema, R. H., Pals, C., Banerji, L., Thomas, N. S., Lam, E. W., Burgering, B. M., Raaijmakers, J. A., Lammers, J. W., Koenderman, L., and Coffer, P. J. (2000) Forkhead transcription factor FKHR-L1 modulates cytokine-dependent transcriptional regulation of $p27^{Kip1}$. *Mol. Cell. Biol.* **20,** 9138–9148
44. Gilley, J., Coffer, P. J., and Ham, J. (2003) FOXO transcription factors directly activate *bim* gene expression and promote apoptosis in sympathetic neurons. *J. Cell Biol.* **162,** 613–622
45. Modur, V., Nagarajan, R., Evers, B. M., and Milbrandt, J. (2002) FOXO proteins regulate tumor necrosis factor-related apoptosis inducing ligand expression. Implications for PTEN mutation in prostate cancer. *J. Biol. Chem.* **277,** 47928–47937
46. Lee, S. S., Kennedy, S., Tolonen, A. C., and Ruvkun, G. (2003) DAF-16 target genes that control *C. elegans* life span and metabolism. *SCIENCE* **300,** 644–647
47. Greer, E. L., and Brunet, A. (2008) FOXO transcription factors in ageing and cancer. *Acta Physiol.* **192,** 19–28
48. Henderson, S. T., and Johnson, T. E. (2001) daf-16 integrates developmental and environmental inputs to mediate aging in the nematode *Caenorhabditis elegans*. *Curr. Biol.* **11,** 1975–1980
49. Brunet, A., Sweeney, L. B., Sturgill, J. F., Chua, K. F., Greer, P. L., Lin, Y., Tran, H., Ross, S. E., Mostoslavsky, R., Cohen, H. Y., Hu, L. S., Cheng, H. L., Jedrychowski, M. P., Gygi, S. P., Sinclair, D. A., Alt, F. W., and Greenberg, M. E. (2004) Stress-dependent regulation of FOXO transcription factors by the SIRT1 deacetylase. *Science* **303,** 2011–2015
50. Martinez, S. C., Tanabe, K., Cras-Méneur, C., Abumrad, N. A., Bernal-Mizrachi, E., and Permutt, M. A. (2008) Inhibition of Foxo1 protects pancreatic islet β-cells against fatty acid and endoplasmic reticulum stress-induced apoptosis. *Diabetes* **57,** 846–859
51. Brunet, A., Bonni, A., Zigmond, M. J., Lin, M. Z., Juo, P., Hu, L. S., Anderson, M. J., Arden, K. C., Blenis, J., and Greenberg, M. E. (1999) Akt promotes cell survival by phosphorylating and inhibiting a Forkhead transcription factor. *Cell* **96,** 857–868
52. Cui, M., Huang, Y., Zhao, Y., and Zheng, J. (2009) New insights for FOXO and cell fate decision in HIV infection and HIV-associated neurocognitive disorder. *Adv. Exp. Med. Biol.* **665,** 143–159
53. Kops, G. J., Dansen, T. B., Polderman, P. E., Saarloos, I., Wirtz, K. W., Coffer, P. J., Huang, T. T., Bos, J. L., Medema, R. H., and Burgering, B. M. (2002) Forkhead transcription factor FOXO3a protects quiescent cells from oxidative stress. *Nature* **419,** 316–321
54. Marinkovic, D., Zhang, X., Yalcin, S., Luciano, J. P., Brugnara, C., Huber, T., and Ghaffari, S. (2007) Foxo3 is required for the regulation of oxidative

stress in erythropoiesis. *J. Clin. Invest.* **117,** 2133–2144
55. Alcendor, R. R., Gao, S., Zhai, P., Zablocki, D., Holle, E., Yu, X., Tian, B., Wagner, T., Vatner, S. F., and Sadoshima, J. (2007) Sirt1 regulates aging and resistance to oxidative stress in the heart. *Circ. Res.* **100,** 1512–1521
56. Burgering, B. M., and Kops, G. J. (2002) Cell cycle and death control. Long live Forkheads. *Trends Biochem. Sci.* **27,** 352–360
57. Furukawa-Hibi, Y., Yoshida-Araki, K., Ohta, T., Ikeda, K., and Motoyama, N. (2002) FOXO Forkhead transcription factors induce G_2-M checkpoint in response to oxidative stress. *J. Biol. Chem.* **277,** 26729–26732
58. Martínez-Gac, L., Marqués, M., García, Z., Campanero, M. R., and Carrera, A. C. (2004) Control of cyclin G_2 mRNA expression by Forkhead transcription factors. Novel mechanism for cell cycle control by phosphoinositide 3-kinase and Forkhead. *Mol. Cell. Biol.* **24,** 2181–2189
59. Medema, R. H., Kops, G. J., Bos, J. L., and Burgering, B. M. (2000) AFX-like Forkhead transcription factors mediate cell cycle regulation by Ras and PKB through $p27^{Kip1}$. *Nature* **404,** 782–787
60. Tran, H., Brunet, A., Grenier, J. M., Datta, S. R., Fornace, A. J., Jr., DiStefano, P. S., Chiang, L. W., and Greenberg, M. E. (2002) DNA repair pathway stimulated by the Forkhead transcription factor FOXO3a through the Gadd45 protein. *Science* **296,** 530–534
61. Kim, G. W., and Chan, P. H. (2001) Oxidative stress and neuronal DNA fragmentation mediate age-dependent vulnerability to the mitochondrial toxin, 3-nitropropionic acid, in the mouse striatum. *Neurobiol. Dis.* **8,** 114–126
62. Nicolson, G. L., Yanagimachi, R., and Yanagimachi, H. (1975) Ultrastructural localization of lectin-binding sites on the zonae pellucidae and plasma membranes of mammalian eggs. *J. Cell Biol.* **66,** 263–274
63. Kajihara, T., Uchino, S., Suzuki, M., Itakura, A., Brosens, J. J., and Ishihara, O. (2009) Increased ovarian follicle atresia in obese Zucker rats is associated with enhanced expression of the Forkhead transcription factor FOXO1. *Med. Mol. Morphol.* **42,** 216–221
64. Burgering, B. M., and Medema, R. H. (2003) Decisions on life and death. FOXO Forkhead transcription factors are in command when PKB/Akt is off duty. *J. Leukoc. Biol.* **73,** 689–701
65. Urbich, C., Knau, A., Fichtlscherer, S., Walter, D. H., Brühl, T., Potente, M., Hofmann, W. K., de Vos, S., Zeiher, A. M., and Dimmeler, S. (2005) FOXO-dependent expression of the proapoptotic protein Bim: pivotal role for apoptosis signaling in endothelial progenitor cells. *FASEB J.* **19,** 974–976
66. Adachi, M., Osawa, Y., Uchinami, H., Kitamura, T., Accili, D., and Brenner, D. A. (2007) The Forkhead transcription factor FoxO1 regulates proliferation and transdifferentiation of hepatic stellate cells. *Gastroenterology* **132,** 1434–1446
67. Matsuda-Minehata, F., Inoue, N., Goto, Y., and Manabe, N. (2006) The regulation of ovarian granulosa cell death by pro- and antiapoptotic molecules. *J. Reprod. Dev.* **52,** 695–705
68. Dlamini, Z., Mbita, Z., and Zungu, M. (2004) Genealogy, expression, and molecular mechanisms in apoptosis. *Pharmacol. Ther.* **101,** 1–15
69. Yuan, H., Zhang, X., Huang, X., Lu, Y., Tang, W., Man, Y., Wang, S., Xi, J., and Li, J. (2010) NADPH oxidase 2-derived reactive oxygen species mediate FFAs-induced dysfunction and apoptosis of β-cells via JNK, p38 MAPK, and p53 pathways. *PLoS One* **5,** e15726
70. Shen, B., Gao, L., Hsu, Y. T., Bledsoe, G., Hagiwara, M., Chao, L., and Chao, J. (2010) Kallistatin attenuates endothelial apoptosis through inhibition of oxidative stress and activation of Akt-eNOS signaling. *Am. J. Physiol. Heart Circ. Physiol.* **299,** H1419–H1427
71. Nemoto, S., and Finkel, T. (2002) Redox regulation of Forkhead proteins through a $p66^{shc}$-dependent signaling pathway. *Science* **295,** 2450–2452
72. Buczyńska, A., and Szadkowska-Stańczyk, I. (2005) Identification of health hazards to rural population living near pesticide dump sites in Poland. *Int. J. Occup. Med. Environ. Health* **18,** 331–339
73. Hoyer, P. B., and Sipes, I. G. (2007) Development of an animal model for ovotoxicity using 4-vinylcyclohexene. A case study. *Birth Defects Res. B Dev. Reprod. Toxicol.* **80,** 113–125
74. Hu, X., Roberts, J. R., Apopa, P. L., Kan, Y. W., and Ma, Q. (2006) Accelerated ovarian failure induced by 4-vinyl cyclohexene diepoxide in Nrf2 null mice. *Mol. Cell. Biol.* **26,** 940–954
75. Grotowski, W., Lecybył, R., Warenik-Szymankiewicz, A., and Trzeciak, W. H. (1997) [The role of apoptosis of granulosa cells in follicular atresia]. *Ginekol Pol.* **68,** 317–326
76. Schiaffonati, L., Rappocciolo, E., Tacchini, L., Cairo, G., and Bernelli-Zazzera, A. (1990) Reprogramming of gene expression in postischemic rat liver. Induction of proto-oncogenes and hsp70 gene family. *J. Cell. Physiol.* **143,** 79–87
77. Salo, D. C., Donovan, C. M., and Davies, K. J. (1991) HSP70 and other possible heat shock or oxidative stress proteins are induced in skeletal muscle, heart, and liver during exercise. *Free Radic. Biol. Med.* **11,** 239–246
78. Mujahid, A., Akiba, Y., and Toyomizu, M. (2007) Acute heat stress induces oxidative stress and decreases adaptation in young white leghorn cockerels by down-regulation of avian uncoupling protein. *Poult. Sci.* **86,** 364–371
79. Silva, J. E. (2006) Thermogenic mechanisms and their hormonal regulation. *Physiol. Rev.* **86,** 435–464
80. Venditti, P., Pamplona, R., Ayala, V., De Rosa, R., Caldarone, G., and Di Meo, S. (2006) Differential effects of experimental and cold-induced hyperthyroidism on factors inducing rat liver oxidative damage. *J. Exp. Biol.* **209,** 817–825
81. Morales, A. E., Pérez-Jiménez, A., Hidalgo, M. C., Abellán, E., and Cardenete, G. (2004) Oxidative stress and antioxidant defenses after prolonged starvation in *Dentex dentex* liver. *Comp. Biochem. Physiol. C Toxicol. Pharmacol.* **139,** 153–161
82. Zafir, A., and Banu, N. (2009) Induction of oxidative stress by restraint stress and corticosterone treatments in rats. *Indian J. Biochem. Biophys.* **46,** 53–58
83. Silva, R. H., Abílio, V. C., Takatsu, A. L., Kameda, S. R., Grassl, C., Chehin, A. B., Medrano, W. A., Calzavara, M. B., Registro, S., Andersen, M. L., Machado, R. B., Carvalho, R. C., Ribeiro Rde, A., Tufik, S., and Frussa-Filho, R. (2004) Role of hippocampal oxidative stress in memory deficits induced by sleep deprivation in mice. *Neuropharmacology* **46,** 895–903